Am J Transl Res 2021;13(11):12421-12430
www.ajtr.org /ISSN:1943-8141/AJTR0137196

*Original Article*

# 17-estradiol nanoparticles influence inflammatory response of myocardial infarction possibly through downregulation of miR-302b

Hao Ma, Dong Xu, Fei Liu, Qing Yao

*Department of Cardiovascular Surgery, Beijing Tiantan Hospital, Capital Medical University, Beijing 100070, China*

Received July 9, 2021; Accepted September 14, 2021; Epub November 15, 2021; Published November 30, 2021

**Abstract:** Cardiovascular death is increasing year by year, and effective treatment is a challenging clinical problem at present. The application of nano materials has pointed to a new therapeutic direction for the clinical treatment of cardiovascular diseases, and preparation of nanoparticles (NPs) with PBCA as carrier material has become a trending spot in clinical research. In this study, we observed the influence of 17-estradiol nanoparticles (17-E2-NPs) on the inflammatory response of myocardial infarction (MI) and its regulatory effect on miR-302b. First of all, we enrolled MI patients and healthy controls, and preliminarily determined that miR-302b was highly expressed in MI and positively correlated with inflammation response. Then, we prepared 17-E2-NPs and purchased rats for modeling to analyze the underlying mechanism of action. The results showed that in rats treated with 17-E2-NPs, the expression of miR-302b and inflammatory cytokines decreased, the proliferation of cardiac fibroblasts reduced and the apoptosis rate increased. According to the above results, we conclude that 17-E2-NPs can inhibit the proliferation of cardiac fibroblasts, promote the apoptosis rate and reduce the inflammatory reaction of MI, via the downregulation of miR-302b, which may be one of the effective treatment schemes for MI in the future.

**Keywords:** 17-estradiol nanoparticles, inflammatory response, miR-302b, myocardial infarction

## Introduction

Myocardial infarction (MI), which accounts for half of cardiovascular deaths [1], is defined as sudden ischemic death of myocardial tissue and is usually caused by coronary artery thrombus occlusion induced by fragile plaque rupture [2, 3]. In addition, ischemia causes significant metabolic and ionic disturbances in the affected myocardium, leading to rapid decline of systolic function [4]. It is shown that smoking, diabetes, dyslipidemia, obesity, unhealthy diet, emotional excitement, and weather changes may all be the predisposing factors of MI [5]. The disease has a sudden and acute attack, which seriously threatens the life of patients [6]. At the present stage, the primary purpose of clinical treatment for MI is to timely dredge the obstructed coronary artery and alleviate ischemia and hypoxia to restore myocardial function [7]. With the increasing accuracy of diagnosis and treatment, the clinical treatment effect has been improved to some extent [8]; nevertheless, challenges for the treatment of MI remain in the face of the numerous factors and complications associated with disease progression.

Increasing evidence suggests that microRNAs (miRNAs) may play an important role in cardiovascular diseases [9]. In particular, miR-302b is one of the most abundant miRNAs in the heart [10]. It is shown that miR-302b is involved in the early pathology of MI and subsequent cardiac remodeling [11]. For example, the research by Xiao et al. shows that miR-302b has a significant effect in modulating myocardial function [12]. Melman proposes that miR-302b plays a key role in gene modulation and is a potential important biomarker for diagnosing MI [13]. In addition, accumulating evidence from epidemiological and cohort studies indicates that endogenous human estrogen (estradiol, E2) and E2 replacement therapy protect women against the progression of cardiovascular disease [14]. And multiple animal studies have

also supported the cardioprotective action of E2 [15]. Furthermore, previous studies have demonstrated that 17-estradiol (E2) protects the liver against I/R injury by reducing microvascular dysfunction and inflammatory responses [16]. Apart from that, the application of nano in clinical medicine is becoming more and more extensive. Nanoparticles (NPs), as a medium between chemical and biological agents, have the advantages of small size, large surface area, simple operation, and rich biological characteristics, which can tailor to various needs [17] to exert positive influence on disease treatment. 17-estradiol nanoparticles (17-E2-NPs) are prepared from polylactic acid-glycolic acid copolymer (PLGA) NPs [18]. Referring to previous data, it is found that PLGA exists in drugs such as irbesartan and has a protective effect on the heart [19]; whereas, no research has demonstrated the effect of 17-E2-NPs on MI. In view of the great clinical challenge of MI, this study investigated the influence of 17-E2-NPs on the inflammatory response of MI. The purpose of this study is to explore the mechanism of the effect of 17-E2-NPs on MI through miR-302b, so as to provide reliable ideas and methods for future clinical diagnosis and treatment of MI.

## Materials and methods

### *Collection of clinical data*

Patients with MI treated in the Beijing Tiantan Hospital from December 2019 to December 2020 were selected to the observation group and those who concurrently underwent physical examination were assigned to the control group. Fasting venous blood was extracted from the two cohorts and stored in a refrigerator at -80°C after centrifugation for testing. The experiment was approved by the ethics committee of our hospital, and all the patients signed the informed consent form.

### *Inclusion and exclusion criteria*

All the included patients met the diagnostic criteria for MI [20] and were treated in our hospital for the first time with complete clinical data and high degree of cooperation. Patients with organ dysfunction, hospital transfer, drug allergy, and recent treatment history such as medication were excluded, as well as those with mental illness. After screening, 63 cases were finally included in observation group. All patients in control group underwent physical examination, with normal examination results. After screening, the number of patients in control group was finally determined to be 75.

### *Animal data*

Forty SD rats, weighing 200-250 g, were purchased from Shanghai Slac Laboratory Animal Co. Ltd. and raised in a light environment of 25-27°C, 60-70% humidity, with food and water available. Twenty rats were randomly selected for modeling, ten for control group, and the other ten were substitution. All animal experiments were carried out with the approval of the relevant ethics committee. The treatment of animals during the experiment was carried out in strict accordance with the relevant regulations on the ca use of experimental animals in the international code of ethics and national health guidelines.

### *Modeling method*

The rats were anesthetized by intraperitoneal injection of 1.2% pentobarbital sodium (50 mg/kg) and placed in the supine position. Then, the chest was bluntly dissected to expose the heart through an incision made between the 3rd and 4th rib of the left chest. The pericardium was cut, and the coronary artery was ligated 2 mm below the left atrial appendage. Modeling was deemed successful if the color of left ventricular anterior wall was gray and purple, with ST segment elevated or t-waves horizontal in ECG. After success in modelling, the incision was sutured layer by layer, and 200,000 IU/kg penicillin was injected locally.

24 h after modeling, rats were anesthetized by intraperitoneal injection of pentobarbital sodium (40 mg/kg) and fixed on the operating table. 2 mL of heart blood was extracted by injection syringe, and serum was obtained after centrifugation for testing. In the process of modeling, there were 4 rats died, and we randomly selected 4 rats from the substitutions to replace the dead ones. The success rate of modeling was about 80%.

### *PCR detection*

Total RNA of the sample to be tested was extracted using Trizol (Thermo Fisher Scientific)

according to the manufacturer's instructions and the cDNA was synthesized using 1 μg of total RNA and TaqMan Reverse Transcription Reagents (Applied Biosystems, Foster City, CA, USA). The PCR cycling began with template denaturation at 95°C for 10 min, followed by 45 cycles of 95°C for 15 sec, 60°C for 60 sec, and 38°C for 5 sec. The primers were: miR-302b: forward: 5'-ATCCAGTGCGTGTCGTG-3'; reverse: 5'-TGCTTAAGTGCTTCCATGTT-3'. U6: forward: 5'-TGCGGGTGCTCGCTTCGGCAGC-3'; reverse: 5'-CCAGTGCAGGGTCCGAGGT-3'. The expression levels relative to U6 were calculated using the formula $2^{-\Delta\Delta CT}$ method.

*Detection of inflammatory cytokines*

Interleukin-6 (IL-6), IL-8 and tumor necrosis factor (TNF-α) were detected using enzyme-linked immunosorbent assay (ELISA) kits purchased from Transgen Biotech Co., Ltd., China.

*17-E2-NP provision*

17-E2 and PLGA (ratio 1:10) were added with dichloromethane-methanol (Fisher Scientific) and dissolved and mixed evenly to prepare a solution containing 3 g/L of PLGA. Then, polyvinyl alcohol (PVA, Sigma) and didodecyldimethylammonium bromide (ratio 3:100, Fisher Scientific) were dissolved in double distilled water to prepare a solution containing 1% polyvinyl alcohol. Thereafter, the above solutions were mixed according to the ratio of 1:3, which were then magnetically stirred, ultrasonically dispersed into nanoemulsions, rotary evaporated, and centrifuged to obtain 17-E2-NPs.

*17-E2-NP preparation results*

17-E2-NPs (300 mg) were dissolved in dichloromethane-absolute ethanol, and the supernatant was obtained after centrifugation. The content of 17-E2 in the samples was determined by high performance liquid chromatography HPLC. HPLC detection information: Acetonitrile-water mixtures (55:45) used as mobile phases; The chromatographic column: TC-$C_{18}$ (250 mm × 50 mm, 5 μm); Measure wavelength: 282 nm; Flow velocity: 1.0 mL/min; Sample size: 10 μL.

The content of 17-E2 in the samples was calculated by comparing the main peak area with that in the standard samples. Drug load = drug content in NPs/NP mass × 100%.

*Determination of in vitro release rate*

17-E2-NPs were dispersed with water for injection, which were then put into a dialysis bag (with a molecular weight of 1200 DA) with both ends clamped. Subsequently, the bag was placed in 5 mL water for injection bath at 37°C and 75 r/m, under constant temperature and oscillation. The samples were taken at 1 h, 2 h, 6 h, 12 h, and 24 h on the first day of release, and then every 24 h. Then all released media were poured out, and equal amounts of fresh media were added. The medium at different time points was determined. The in vitro release rate of 17-E2-NPs was drawn by fitting the equation of cumulative release and time.

*17-E2-NP intervention in rats*

Ten modeled rats were randomly selected for 17-E2-NP intervention 72 h after operation and were set as the intervention group; the other ten untreated rats were in the model group. Rats in the intervention group were injected with 17-E2-NPs (4 mg/100 g) at the edge of heart infarction area, while those in the model group were injected with the same amount of normal saline.

*MI area detection*

Four weeks after injection, the rats were killed by dislocation of cervical vertebra under anesthesia by intraperitoneal injection of pentobarbital sodium (40 mg/kg), and the infarcted tissues were obtained, dehydrated, embedded in paraffin, and the slices were cut at 4 μm thickness. HE staining was performed to observe the inflammatory cell infiltration after myocardial infarction.

TTC staining was used to detect myocardial infarction area: ventricles were cut horizontally along the longitudinal axis of the heart with a thickness of about 2 mm, immersed in phosphoric acid buffer containing 1% TTC, incubated at 37°C for 20 min away from light, and fixed in 4% paraformaldehyde for 40 min. The myocardial tissue sections were dried to observe the staining condition and photographed. Image J software was used to process the images and calculate the infarct area of myocardial tissue. The non-infarct area was dark red, and the infarct area was white.

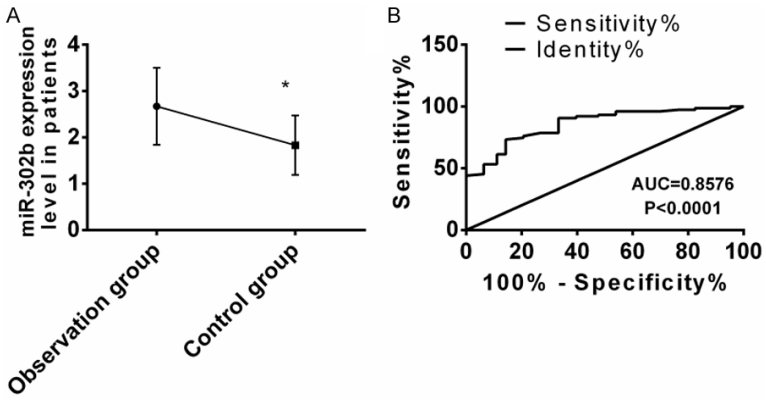


**Figure 1.** Expression and clinical significance of miR-302b. A. miR-302b expression. B. ROC curve of miR-302b in predicting MI. *$P$<0.05.

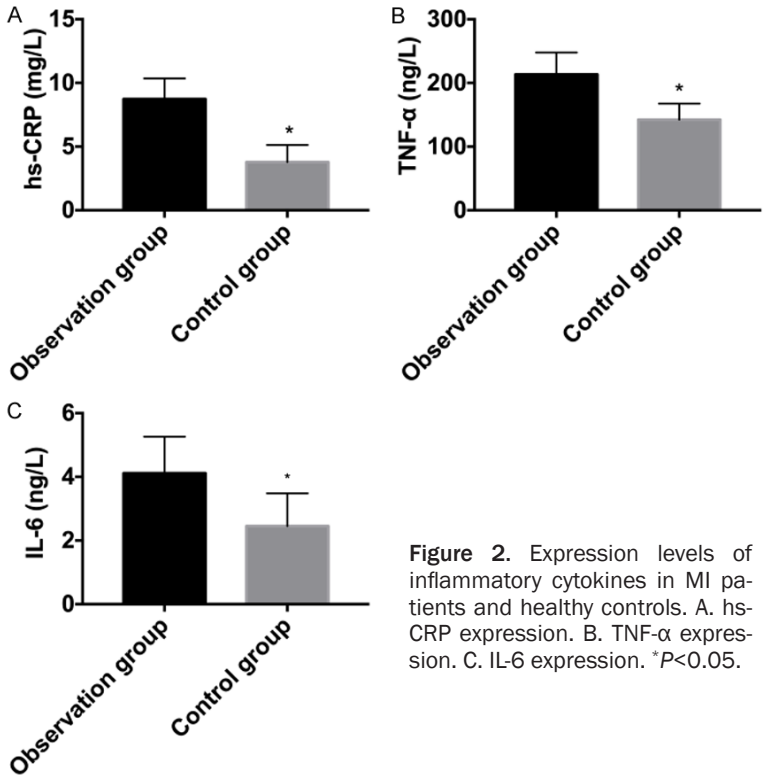


**Figure 2.** Expression levels of inflammatory cytokines in MI patients and healthy controls. A. hs-CRP expression. B. TNF-α expression. C. IL-6 expression. *$P$<0.05.

*Cultivation of rat cardiac fibroblasts*

Rat heart tissue (100 mg) was cut into pieces, digested with 1 g/L pancreatin (Sigma-Aldrich) and 0.8 g/L collagenase IV (Sigma-Aldrich), and cultured in 10% fetal bovine serum medium. They were then digested on a shaking table at 37°C and 200 r/min. After digestion, the cells were gently pipetted with sterile straws and mixed, and added with equal volume of 10% FBS HG/DMEM (Gibco) to terminate. The above procedures were repeated, and the cells were pipetted and mixed repeatedly in the diameter of 10 cm cell dishes containing 0.1% gelatin. Then the cell dishes were placed in an incubator at 37°C and 5% $CO_2$ for differential adherence for 60-90 min [21]. The adherent cells are cardiac fibroblasts. The non-adherent cardiomyocytes, blood cells and endothelial cells were discarded. Thereafter, 10 mL Hg/DMEM containing 10% FBS was added again, and the solution was changed every 1 day. Immunofluorescence staining determined that the purity of cardiac fibroblasts was above 93%. The cells were immediately used for follow-up tests.

The identification of myocardial fibroblasts was done by vimentin immunofluorescence staining: Myocardial primary fibroblasts were inoculated into 6-well plates with sterile cover glass, then fixed with 4% paraformaldehyde for 30 min and washed with 0.01 mmol/L PBS for 3 times (2 min each time). Cells were then treated at room temperature for 30 min with 0.2% Triton X-100, and Washed with 0.01 mmol/L PBS for 3 times (2 min each time). They were then blocked with 200 μL non-immune animal serum at room temperature for 30 min, and incubated with specific primary antibodies against vimentin (Cell signaling technology, 1:100) for overnight at 4°C. After 30 min at room temperature the next day, they were washed with 0.01 mmol/L PBS for 3 times (2 min each time), and then added with 200 μL TRITC labeled secondary antibody (Santa Cruz Biotechnology, 1:100), incubated at room temperature in the dark for 1.5 h, washed with 0.01 mmol/L PBS for 3 times (2 min each time), and sealed with glycerol after DAPI staining. The number of positive

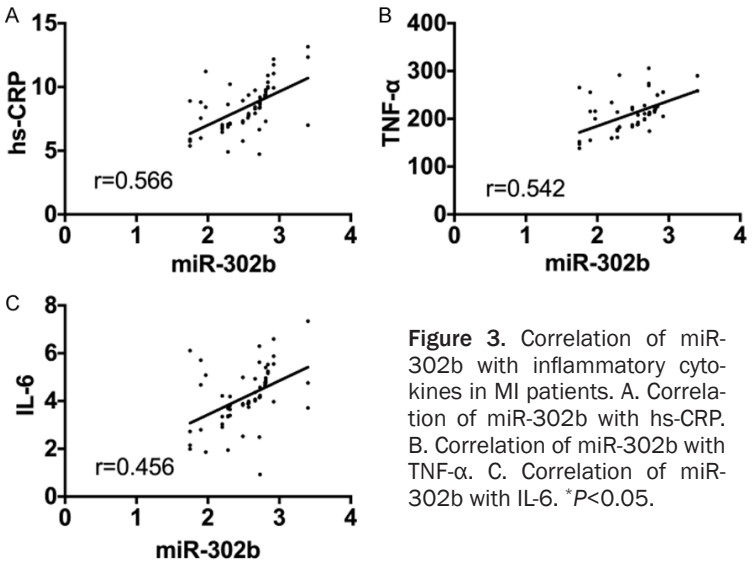


**Figure 3.** Correlation of miR-302b with inflammatory cytokines in MI patients. A. Correlation of miR-302b with hs-CRP. B. Correlation of miR-302b with TNF-α. C. Correlation of miR-302b with IL-6. *$P$<0.05.

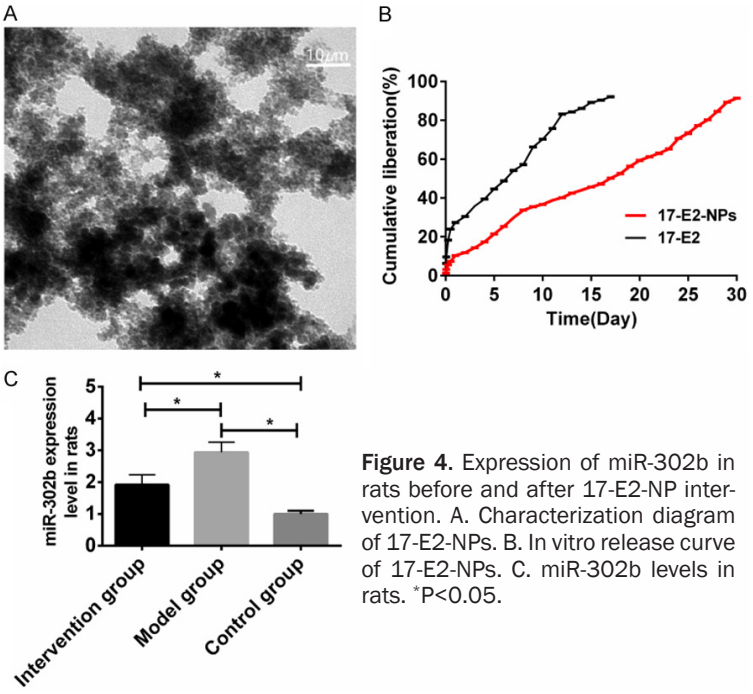


**Figure 4.** Expression of miR-302b in rats before and after 17-E2-NP intervention. A. Characterization diagram of 17-E2-NPs. B. In vitro release curve of 17-E2-NPs. C. miR-302b levels in rats. *P<0.05.

cells was observed and counted under fluorescence microscope.

*Cell proliferation detection*

After subculture, rat cardiac fibroblasts were inoculated in 96-well plate for 12, 24, 48 and 72 h of cultivation, and then CCK-8 reagent (Dojindo Laboratories, Kumamoto, Japan) was added to incubate cells for 1 hour. Then, absorbance value at 450 nm was determined using a microplate reader.

*Apoptosis detection*

The cells were digested with enzyme-free digestive solution and adjusted to 1 × $10^6$ cells/mL. AnnexinV-FITC and PI were added at 1 μL each. After incubation for 30 min, the cells were resuspended in PBS, and the apoptosis rate was detected by Flow cytometry. AnnexinV/PI apoptosis kit was purchased from Shanghai Majorbio Biotech Co. Ltd., China.

*Statistical processing*

Statistical Product and Service Solutions (SPSS 23.0) software was used for statistical analysis. Experimental data were expressed as mean ± SD. The unpaired t-test or a two-tailed Mann-Whitney test was used to compare the differential expression of serum miRNAs and inflammatory cytokine levels between MI patients and control patients. The difference among groups of rats was assessed by one-way AVONA followed with Bonferroni post-hoc test. Area under curve (AUC) was used as the evaluation criteria and Pearson's correlation was used for correlation analysis. P<0.05 was considered as significant difference.

## Results and discussion

*Expression and clinical significance of miR-302b*

The expression of miR-302b was significantly increased in MI patients than in controls ($P$<0.05, **Figure 1A**). ROC curve analysis determined that when miR-302b <2.19, the sensitivity and specificity of predicting MI were 73.33% and 85.71% respectively (**Figure 1B**).

*Expression of inflammatory cytokines*

Measurements of inflammatory cytokines revealed that the levels of hs-CRP, TNF-α and IL-6

**Table 1.** Particle diameter, PDI, and zeta potential

| | Particle diameter (nm) | PDI | Zeta potential (mV) |
|---|---|---|---|
| 17-E2-NPs | 192±7 | 0.164±0.011 | -37.4±1.7 |

**Table 2.** Drug loading measurement results

| Lot number | Encapsulation efficiency (%) | Drug loading (%) |
|---|---|---|
| 20190712-1 | 86.34 | 4.03 |
| 20190712-2 | 85.87 | 3.91 |
| 20190712-3 | 83.28 | 3.84 |
| | 85.16±1.65 | 3.93±0.93 |

were significantly higher in the observation group compared with those of the control group ($P$<0.05, **Figure 2**).

*Correlation of miR-302b expression with inflammatory cytokines in the observation group*

Pearson correlation coefficient was used to analyze the correlation of miR-302b with inflammatory cytokines in the observation group. It showed that the expression level of miR-302b was positively associated with the level of hs-CRP, TNF-α and IL-6 (r=0.566, r=0.542, r=0.456, **Figure 3**).

*Expression of miR-302b in rats before and after 17-E2-NP intervention*

Under TEM, 17-E2-NPs had a diameter of about 200 nm with a circular spherical distribution and relatively uniform dispersion (**Figure 4A**). The zeta potential values greater than u30 mV indicate a high stability of the nanoparticle systems due to effective electrostatic particle repulsion (**Table 1**). The encapsulation efficiency and drug load of 17-E2 were 85.16 load and 3.936 load % (**Table 2**). In vitro release curve of 17-E2-NPs showed that the higher release rate in the first 10 days may be related to the partial melting of 17-E2 on the surface of NPs. From Day 10 to Day 30, the increase of release rate decreased slightly. The cumulative release rate was close to 100% at Day 30, and the release of 17-E2 (free-drug) was rapid - 90.34% was released within 16 days. The results showed that the 17-E2-NPs has good sustained release properties (**Figure 4B**). miR-302b declined dramatically in rats after 17-E2-NP intervention (**Figure 4C**).

*Levels of inflammatory cytokines in rats before and after 17-E2-NP intervention*

Measurements of inflammatory cytokine levels identified reduced hs-CRP, TNF-α and IL-6 levels in rats following 17-E2-NP intervention (**Figure 5**).

*MI area in rats*

HE staining was used to determine myocardial pathology (**Figure 6A**). Myocardial cells in the model group were loosely connected and partially disordered, and interstitial inflammatory exudation significantly increased. Myocardial cells in the intervention group were organized more orderly and interstitial inflammatory exudation decreased. TTC staining was used to calculate the MI area. After comparison, it was found that the MI area in 17-E2-NPs intervened rats was statistically smaller than that in non-intervened rats ($P$<0.05, **Figure 6B**).

*Effect of 17-E2-NPs on cardiac fibroblasts*

According to the characteristics of proteins contained in cardiac fibroblasts, Vimentin was used as an indicator of cardiac fibroblast detection and identification. The immunofluorescence staining determined that most of the cells showed positive reaction and positive cell rate for more than 93% (**Figure 7A**). The expression of miR-302b in cardiac fibroblasts in the intervention group decreased evidently as compared to the model group ($P$<0.05, **Figure 7B**). *In vitro* experiments showed that compared with the model group, the proliferation of cardiac fibroblasts in the intervention group was lower ($P$<0.05, **Figure 7C**), while the apoptosis rate was higher ($P$<0.05, **Figure 7D**).

## Discussion

MI is a leading cause of morbidity and mortality worldwide [22]. Infarcted hearts exhibit a typical cascade reaction of cell death characterized by cardiomyocyte loss and fibrotic scarring [23]. Cardiac hypertrophy and fibrosis are prone to cause ventricular wall thickening and stiffness, which together result in unfavorable car-

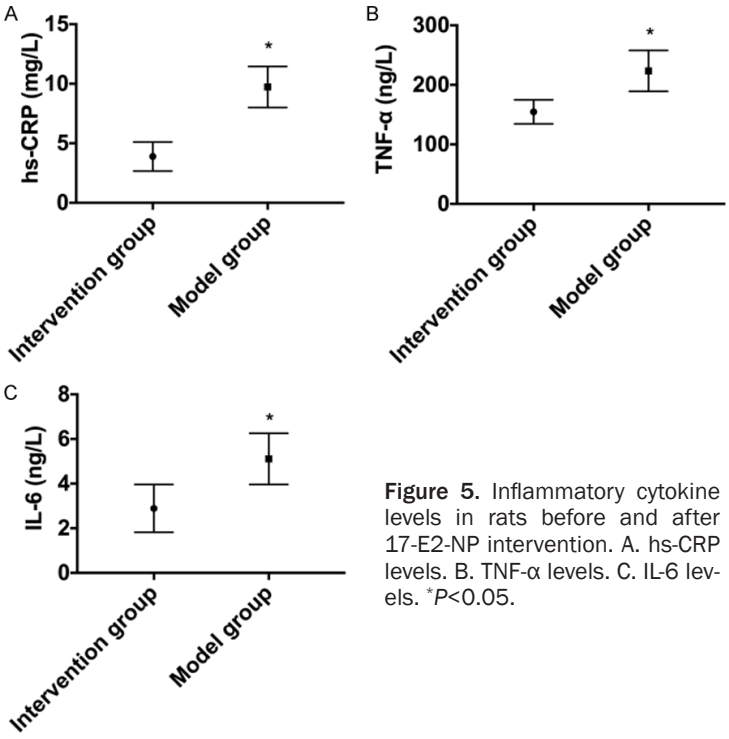


**Figure 5.** Inflammatory cytokine levels in rats before and after 17-E2-NP intervention. A. hs-CRP levels. B. TNF-α levels. C. IL-6 levels. $^{*}P<0.05$.

diac remodeling, ultimately leading to impaired cardiac function and subsequent heart failure [24]. Therefore, strategies that facilitate smooth treatment rather than hindering heart remodeling may be effective treatments for MI. NPs are drug-carrying particles made of natural polymers or synthetic chemicals [25], which have targeting properties and many advantages such as slow release, drug protection, and capability of improving therapeutic efficacy [26]. In view of the limitations in the current treatment of MI and the promising application prospect of NPs, we conducted an in-depth study on the influence of 17-E2-NPs on the inflammatory response of MI through miR-302b.

In this study, MI patients and healthy subjects were included to preliminarily understand the expression and clinical significance of miR-302b in patients. The results revealed that the expression of miR-302b was increased in cases and had good clinical diagnostic value for MI, suggesting its involvement in the occurrence and development of MI. Previously, the study of Jia et al. confirmed that miR-302b showed high expression in patients with MI [27], which can support our experimental results. At present, the clinical diagnosis of MI is mainly based on imaging technology, which is time-consuming and has the risk of misdiagnosis [28]. On the contrary, the detection of serum markers is more convenient, fast, and easy to preserve compared to imaging technology, which will bring more convenient diagnostic methods to clinical diagnosis and treatment. Evidently higher levels of hs-CRP, TNF-α and IL-6 were determined in cases than in controls in our research. Inflammatory cytokines can directly damage endothelial function and lead to atherosclerosis [29], which is closely related to vascular endothelial damage and functional changes [30]. It also suggests that effective control of inflammatory response has a positive effect on the treatment of patients with MI. Through correlation analysis, we observed that the expression of miR-302b in MI patients is consistent with the expression trend of inflammatory cytokines. From the above, we preliminarily confirmed that miR-302b participates in the occurrence and development of MI; however, the specific influencing mechanism of 17-E2-NPs on the inflammatory response of MI through miR-302b is still unclear. Therefore, we prepared 17-E2-NPs and purchased SD rats for modeling and biological analysis. First, we detected the properties of 17-E2-NPs. Under TEM, 17-E2-NPs had a particle size of approximately 200 nm with uniform distribution. Subsequently, we injected 17-E2-NPs into the edge of the infarct area of rats in the intervention group for analyses. The measurement of miR-302b before and after intervention revealed profoundly decreased miR-302b after 17-E2-NP intervention. Also, the levels of inflammatory cytokines hs-CRP, TNF-α and IL-6 were found to be significantly reduced in rats intervened by 17-E2-NPs compared with those without intervention. It further indicates that 17-E2-NP intervention can effectively inhibit inflammatory cytokines and improve vascular endothelial function in rats, demonstrating that 17-E2-NP intervention may play a certain role in the clinical treatment of MI [31]. We also observed the MI area of rats in the intervention group and the model group. The results showed that the MI area of rats treated with 17-E2-NPs was significantly small-

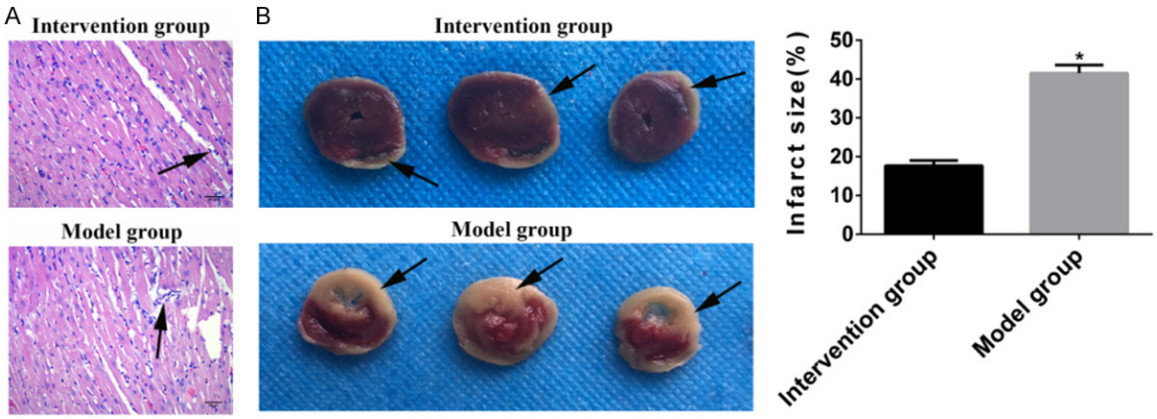


**Figure 6.** Myocardial infarction area of the two groups of rats. A. HE staining (the arrows point to the interstitial inflammatory exudate). B. TTC staining (the arrows point to infarct site). *$P$<0.05.

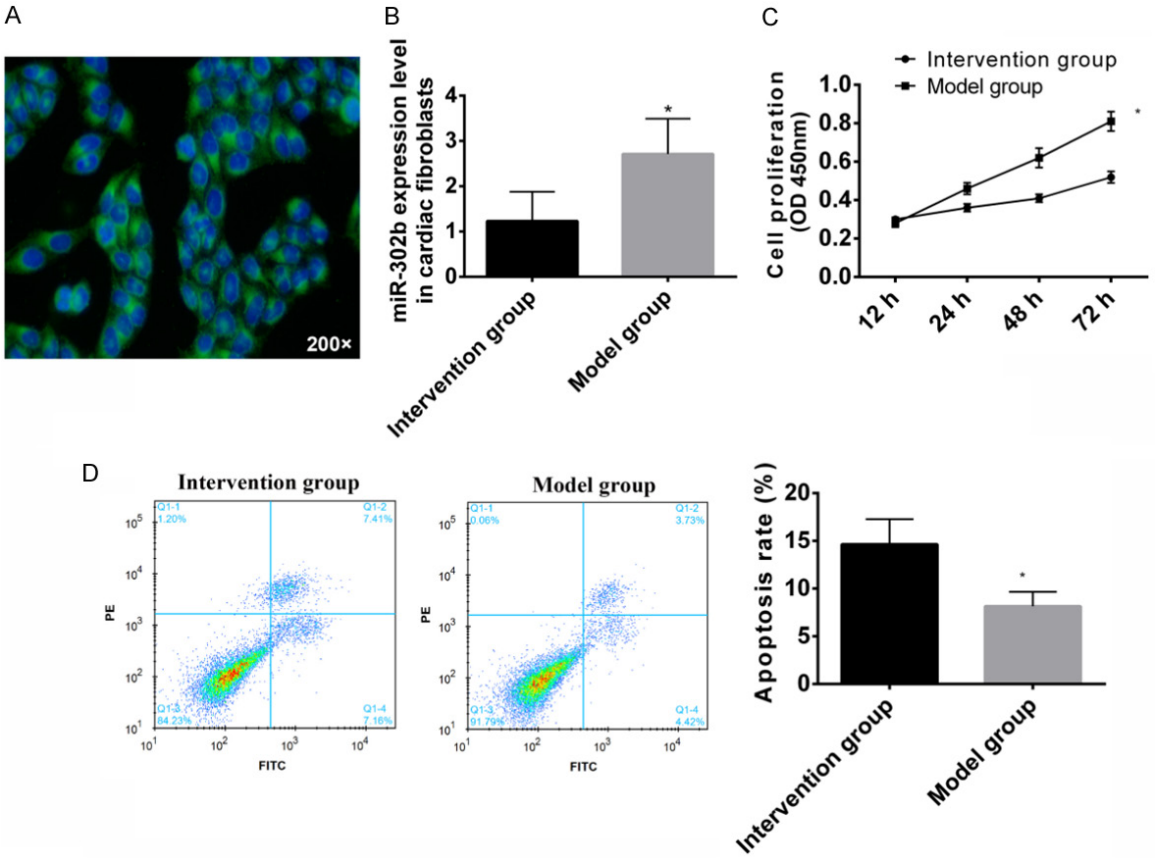


**Figure 7.** Effect of 17-E2-NPs on cardiac fibroblasts. A. Immunofluorescence staining. B. miR-302b levels in rat cardiac fibroblasts. C. Cell proliferation. D. Apoptosis. *$P$<0.05.

er than that of rats without intervention, which finding confirmed our initial hypothesis that 17-E2-NP injection into the infarct area of rat heart has an effective therapeutic effect. Finally, we analyzed the effect of 17-E2-NPs on rat cardiac fibroblasts. The detection of miR-302b expression revealed that the expression of miR-302b in the intervention group was significantly lower than that in the model group, indicating that 17-E2-NPs can affect miR-302b

expression in MI. *In vitro* experiments showed that compared with the model group, the proliferation of cardiac fibroblasts was lower, and the apoptosis rate was higher in the intervention group. The ability of cardiac fibroblasts to colonize, differentiate, migrate and produce collagen plays a key role in the process of cardiac fibrosis. Excessive proliferation of cardiac fibroblasts can also lead to myocardial fibrosis. In the process of cardiac extracellular matrix remolding, cardiac fibroblasts are differentiated into myogenic fibroblasts to increase their colloid synthesis power, and the colonization and migration power of cardiac fibroblasts are enhanced to increase the number of cells in myocardial stem or remolding area. Previous researches have pointed out that miR-302b has a significant promoting effect on MI, which was consistent with our above experimental results that the expression of miR-302b elevated as the levels of inflammatory cytokines increased, suggesting that 17-E2-NPs could influence the inflammatory response of MI, which might be through modulating miR-302b expression.

This investigation initially confirmed the clinical implications of miR-302b in MI. However, there are still some shortcomings in this study. Generally speaking, the analysis of ROC needs to include as much patient data as possible for statistical analysis. Whereas, the number of cases included in this study is relatively small, which may lead to the inability to obtain the most accurate results. Besides, we are unable to analyze the long-term prognosis of miR-302b in patients with MI due to the short timeframe. Moreover, as indicated by the literature [32], the occurrence of MI is a complex process influenced by multiple genes and pathways, so further exploration and discussion regarding the mechanism of miR-302b involvement in MI are warranted. We will launch more comprehensive experiments and analysis to address the above deficiencies.

## Conclusion

17-E2-NPs can inhibit the proliferation, promote the apoptosis rate of cardiac fibroblasts and reduce the inflammatory response of MI, which might be mediated by the regulation of the expression level of miR-302b. This may be one of the effective schemes for future treatment of MI.

## Disclosure of conflict of interest

None.

**Address correspondence to:** Hao Ma, Department of Cardiovascular Surgery, Beijing Tiantan Hospital, Capital Medical University, No. 119, South 4 Ring West Road, Feng Tai District, Beijing, China. Tel: +86-13701165716; E-mail: mah197608@163.com

## References

[1] Reed GW, Rossi JE and Cannon CP. Acute myocardial infarction. Lancet 2017; 389: 197-210.
[2] Saleh M and Ambrose JA. Understanding myocardial infarction. F1000Res 2018; 7: F1000 Faculty Rev-1378.
[3] Anderson JL and Morrow DA. Acute myocardial infarction. N Engl J Med 2017; 376: 2053-2064.
[4] Ramachandra CJ, Hernandez-Resendiz S, Crespo-Avilan GE, Lin YH and Hausenloy DJ. Mitochondria in acute myocardial infarction and cardioprotection. EBioMedicine 2020; 57: 102884.
[5] Thygesen K, Alpert JS, Jaffe AS, Chaitman BR, Bax JJ, Morrow DA and White HD; Executive Group on behalf of the Joint European Society of Cardiology (ESC)/American College of Cardiology (ACC)/American Heart Association (AHA)/World Heart Federation (WHF) Task Force for the Universal Definition of Myocardial Infarction. Fourth universal definition of myocardial infarction (2018). Circulation 2018; 138: e618-e651.
[6] Tibaut M, Mekis D and Petrovic D. Pathophysiology of myocardial infarction and acute management strategies. Cardiovasc Hematol Agents Med Chem 2017; 14: 150-159.
[7] Sandoval Y and Jaffe AS. Type 2 myocardial infarction: JACC review topic of the week. J Am Coll Cardiol 2019; 73: 1846-1860.
[8] Harrington DH, Stueben F and Lenahan CM. ST-elevation myocardial infarction and Non-ST-elevation myocardial infarction: medical and surgical interventions. Crit Care Nurs Clin North Am 2018; 31: 49-64.
[9] Xiao Y, Zhao J, Tuazon JP, Borlongan CV and Yu G. MicroRNA-133a and myocardial infarction. Cell Transplantation 2019; 28: 831-838.
[10] Yang S, Fu C, Xu R, Xun Z, Zhao X and Fang R. Serum microRNA-302b: the novel biomarker for diagnosis of acute myocardial infarction. Br J Biomed Sci 2017; 74: 214-216.
[11] Li G, Song Y, Li YD, Jie LJ, Wu WY, Li JZ, Zhang Q and Wang Y. Circulating miRNA-302 family members as potential biomarkers for the diagnosis of acute heart failure. Biomark Med 2018; 12: 871-880.

[12] Xiao J, Gao R, Bei Y, Zhou Q, Zhou Y, Zhang H, Jin M, Wei S, Wang K, Xu X, Yao W, Xu D, Zhou F, Jiang J, Li X and Das S. Circulating miR-30d predicts survival in patients with acute heart failure. Cell Physiol Biochem 2017; 41: 865-874.

[13] Melman YF, Shah R, Danielson K, Xiao J, Simonson B, Barth A, Chakir K, Lewis GD, Lavender Z, Truong QA, Kleber A, Das R, Rosenzweig A, Wang Y, Kass D, Singh JP and Das S. Circulating MicroRNA-30d is associated with response to cardiac resynchronization therapy in heart failure and regulates cardiomyocyte apoptosis: a translational pilot study. Circulation 2015; 131: 2202-2216.

[14] Koledova VV and Khalil RA. Sex hormone replacement therapy and modulation of vascular function in cardiovascular disease. Expert Rev Cardiovasc Ther 2007; 5: 777-789.

[15] Yu HP, Hsieh YC, Suzuki T, Choudhry MA, Schwacha MG, Bland KI and Chaudry IH. The PI3K/Akt pathway mediates the nongenomic cardioprotective effects of estrogen following trauma-hemorrhage. Ann Surg 2007; 245: 971.

[16] Burkhardt M, Slotta J, Garcia P, Seekamp A, Menger M and Pohlemann T. The effect of estrogen on hepatic microcirculation after ischemia/reperfusion. Int J Colorectal Dis 2008; 23: 113-119.

[17] Dadfar SM, Roemhild K, Drude NI, von Stillfried S, Knüchel R, Kiessling F and Lammers T. Iron oxide nanoparticles: diagnostic, therapeutic and theranostic applications. Adv Drug Deliv Rev 2019; 138: 302-325.

[18] Sadat Tabatabaei Mirakabad F, Nejati-Koshki K, Akbarzadeh A, Yamchi MR, Milani M, Zarghami N, Zeighamian V, Rahimzadeh A, Alimohammadi S, Hanifehpour Y and Joo SW. PLGA-based nanoparticles as cancer drug delivery systems. Asian Pac J Cancer Prev 2014; 15: 517-535.

[19] Oduk Y, Zhu W, Kannappan R, Zhao M, Borovjagin AV, Oparil S and Zhang JJ. VEGF nanoparticles repair the heart after myocardial infarction. Am J Physiol Heart Circ Physiol 2018; 314: H278-H284.

[20] Thygesen K, Alpert JS, White H and Joint E; Joint ACC/AHA/WHF Task Force for the Redefinition of Myocardial Infarction. Universal definition of myocardial infarction. Eur Heart J 2007; 28: 2525-2538.

[21] Tian K, Liu Z, Wang J, Xu S, You T and Liu P. Sirtuin-6 inhibits cardiac fibroblasts differentiation into myofibroblasts via inactivation of nuclear factor κB signaling. Transl Res 2015; 165: 374-386.

[22] Johansson S, Rosengren A, Young K and Jennings E. Mortality and morbidity trends after the first year in survivors of acute myocardial infarction: a systematic review. BMC Cardiovasc Disord 2017; 17: 53.

[23] Khodayari S, Khodayari H, Amiri AZ, Eslami M, Farhud D, Hescheler J and Nayernia K. Inflammatory microenvironment of acute myocardial infarction prevents regeneration of heart with stem cells therapy. Cell Physiol Biochem 2019; 53: 887-909.

[24] Kapur NK, Thayer KL and Zweck E. Cardiogenic shock in the setting of acute myocardial infarction. Methodist Debakey Cardiovasc J 2020; 16: 16-21.

[25] Mottaghitalab F, Farokhi M, Fatahi Y, Atyabi F and Dinarvand R. New insights into designing hybrid nanoparticles for lung cancer: diagnosis and treatment. J Control Release 2019; 295: 250-267.

[26] Ernsting MJ, Murakami M, Roy A and Li SD. Factors controlling the pharmacokinetics, biodistribution and intratumoral penetration of nanoparticles. J Control Release 2013; 172: 782-794.

[27] Jia K, Shi P, Han X, Chen T, Tang H and Wang J. Diagnostic value of miR-30d-5p and miR-125b-5p in acute myocardial infarction. Mol Med Rep 2016; 14: 184-194.

[28] Lu L, Liu M, Sun R, Zheng Y and Zhang P. Myocardial infarction: symptoms and treatments. Cell Biochem Biophys 2015; 72: 865-867.

[29] Prabhu SD and Frangogiannis NG. The biological basis for cardiac repair after myocardial infarction: from inflammation to fibrosis. Circ Res 2016; 119: 91-112.

[30] Rischpler C. Acute myocardial infarction. Q J Nucl Med Mol Imaging 2016; 60: 236-251.

[31] Bejarano J, Navarro-Marquez M, Morales-Zavala F, Morales JO, Garcia-Carvajal I, Araya-Fuentes E, Flores Y, Verdejo HE, Castro PF, Lavandero S and Kogan MJ. Nanoparticles for diagnosis and therapy of atherosclerosis and myocardial infarction: evolution toward prospective theranostic approaches. Theranostics 2018; 8: 4710-4732.

[32] Curley D, Plaza BL, Shah AM and Botnar RM. Molecular imaging of cardiac remodelling after myocardial infarction. Basic Res Cardiol 2018; 113: 10.